



Spatial attention boosts short-latency neural responses in human visual cortex

Jyoti Mishra^a, Antígona Martínez^{b,c}, Charles E. Schroeder^c, Steven A. Hillyard^{b,*}

^a Department of Neurology and Physiology, Keck Center for Integrative Neurosciences, University of California, San Francisco, San Francisco, CA 94158, United States

^b Department of Neurosciences, University of California, San Diego, La Jolla, CA 92093, United States

^c Nathan S. Kline Institute for Psychiatric Research, Orangeburg, NY 10962, United States

ARTICLE INFO

Article history:

Received 23 May 2011

Revised 8 August 2011

Accepted 12 September 2011

Available online 1 October 2011

Keywords:

ERPs

EEG synchrony

Spatial attention

Theta

Alpha

ABSTRACT

In a previous study of visual–spatial attention, Martínez et al. (2007) replicated the well-known finding that stimuli at attended locations elicit enlarged early components in the averaged event-related potential (ERP), which were localized to extrastriate visual cortex. The mechanisms that underlie these attention-related ERP modulations in the latency range of 80–200 ms, however, remain unclear. The main question is whether attention produces increased ERP amplitudes in time-domain averages by augmenting stimulus-triggered neural activity, or alternatively, by increasing the phase-locking of ongoing EEG oscillations to the attended stimuli. We compared these alternative mechanisms using Morlet wavelet decompositions of event-related EEG changes. By analyzing single-trial spectral amplitudes in the theta (4–8 Hz) and alpha (8–12 Hz) bands, which were the dominant frequencies of the early ERP components, it was found that stimuli at attended locations elicited enhanced neural responses in the theta band in the P1 (88–120 ms) and N1 (148–184 ms) latency ranges that were additive with the ongoing EEG. In the alpha band there was evidence for both increased additive neural activity and increased phase-synchronization of the EEG following attended stimuli, but systematic correlations between pre- and post-stimulus alpha activity were more consistent with an additive mechanism. These findings provide the strongest evidence to date in humans that short-latency neural activity elicited by stimuli within the spotlight of spatial attention is boosted or amplified at early stages of processing in extrastriate visual cortex.

© 2011 Elsevier Inc. All rights reserved.

Introduction

Voluntarily directing attention to a particular location in visual space improves the detection and discrimination of stimuli at that location (reviewed in Wright and Ward, 2008). Electrophysiological studies of visual–spatial attention in humans have consistently shown that stimuli at attended locations elicit enlarged P1 (80–130 ms) and N1 (130–200 ms) components in the event-related potential (ERP), which have been localized to neural generators in extrastriate visual cortex (Di Russo et al., 2003; Martínez et al., 1999, 2006; Noesselt et al., 2002). Neurophysiological recordings in non-human primates have demonstrated similarly strong influences of top-down attentional control over stimulus-elicited neural activity in homologous extrastriate visual areas (e.g. Lee et al., 2007; Reynolds, 2004).

The present study investigates the mechanisms responsible for the attention-related enhancement of the early components of the visual ERP in humans. Some recent studies that combined frequency and time domain analyses have suggested that ERP components emerge in the averaged waveform because the stimulus resets or synchronizes

the phase of the ongoing EEG oscillations in a consistent way (Gruber et al., 2005; Hanslmayr et al., 2007; Jansen et al., 2003; Klimesch et al., 2007; Makeig et al., 2002). A number of other studies, however, have shown that such a phase synchronization mechanism does not adequately account for many types of ERPs (Becker et al., 2008; Fell et al., 2004; Mäkinen et al., 2005; Mazaheri and Jensen, 2006; Min et al., 2007; Shah et al., 2004). These latter studies provide support for the alternative hypothesis that ERPs originate at least in part from stimulus-triggered neural activity and synaptic currents that are additive with the ongoing oscillations of the EEG. Attention-related increases in averaged ERP amplitudes have generally been attributed to such additive neural activity, either produced by an increase in the gain or amplification of attended sensory input or by the triggering of new neural activity in attention-specific circuits (reviewed in Hillyard and Anllo-Vento, 1998; Hopf et al., 2009).

The present study investigated these alternative mechanisms of “phase-synchronization” and “added-activity” for producing attention-related increases in early ERP components in a spatial attention task previously reported by Martínez et al. (2007). Single-trial wavelet decomposition was carried out to assess changes in event-related neural activity following presentation of attended and unattended stimuli. If the attention-related increases in P1–N1 amplitudes in the averaged ERP waveforms were produced by the triggering of additive neural activity, the single trial wavelet analysis would show increased spectral

* Corresponding author at: University of California, San Diego, Dept. of Neurosciences 0608, 9500 Gilman Drive, La Jolla, CA 92093-0608, United States. Fax: +1 858 534 1566. E-mail address: shillyard@ucsd.edu (S.A. Hillyard).

amplitudes measured in the relevant frequency bands. This amplitude increase would be accompanied by an increase in phase consistency over trials, assuming that the additive neural activity had a consistent waveform. Alternatively, if the averaged P1–N1 amplitude increases caused by attention were produced solely by phase-synchronization, the single trial analysis would show an increase in phase consistency over trials without any increase in additive spectral amplitude. The present wavelet analyses showed that the increase in early visual ERP amplitudes produced by spatial attention was associated with a substantial increase in additive event-related neural activity and could not be accounted for solely by a mechanism of phase synchronization.

Materials and methods

Task and stimuli

The present study reports additional analyses that were carried out in the frequency domain of the EEG/ERP data obtained in a visual-spatial attention experiment previously reported by [Martinez et al. \(2007\)](#). Fourteen healthy volunteers (mean age, 21 years; nine females) participated in the study. All subjects were right handed, had normal or corrected-to-normal vision, and gave informed consent to participate in the experiment.

The stimuli in this experiment were either a single white square ($6.5 \times 6.5^\circ$ visual angle) on a gray background [intact object (IO) condition] or four separated rectangular white shapes [fragmented object (FO) condition] that together comprised the same area as the single square ([Fig. 1](#) reproduced with permission from [Martinez et al., 2007](#)). All stimuli were white on a gray background and contained a small fixation cross in the center that was present at all times. In both the IO and FO configurations, task stimuli consisted of brief (100 ms) offsets of the corners in either the upper left (UL), upper right (UR), lower left (LL), or lower right (LR) quadrants. Corner offsets left either a concave edge (standards, $p = 0.8$) or a convex edge (targets, $p = 0.2$) and occurred in random order, one at a time, in the different quadrants at intervals of 400–600 ms. Stimuli were delivered in 20 s blocks with either the IO or FO configuration. In both cases, subjects were instructed to maintain fixation on the central

cross while directing attention to the corner (quadrant) indicated by a pair of arrows presented just above or below fixation. Subjects were instructed to respond as quickly and accurately as possible to target stimuli appearing in the attended quadrant and to ignore all stimuli at the other quadrants. All subjects responded with their right hand. A single run consisted of five attend-left blocks and five attend-right blocks. During half of the runs, the cues alternated between the UL and UR quadrants and in the remaining half between the LL and LR quadrants. Each subject took part in a total of 20 runs resulting in ~500 stimuli being presented in each condition (~250 each in IO/FO). The order of conditions (attend upper field or lower field and IO or FO) was counterbalanced across subjects.

Electrophysiological recordings

Subjects sat in a dimly lit recording chamber and viewed the stimuli on a video monitor at a distance of 100 cm. Recordings were acquired from 62 scalp electrodes using a modified 10–20 system montage ([Di Russo et al., 2003](#)) referenced to the right mastoid. Eye movements and blinks were monitored via recordings of the horizontal (right vs. left outer canthi) and vertical (below the eye vs. right mastoid) electro-oculogram (EOG). The EEG was digitized at 250 Hz with an amplifier bandpass of 0.1–80 Hz. Computerized artifact rejection was performed to discard epochs in which deviations in eye position and/or blinks (defined as any peak-to-peak amplitude change of $\geq 60 \mu\text{V}$ in the EOG channels) or amplifier blocking (defined as a flat voltage line for ≥ 40 ms) occurred. Approximately 10% of all trials were rejected based on these criteria.

While the design of the [Martinez et al. \(2007\)](#) study was aimed at revealing object-selective ERP effects by comparing attention-related ERP modulations in the IO and FO conditions, the present analysis was exclusively focused on spatial attention effects. Accordingly, the influence of spatial attention on visual ERPs was analyzed here only in the IO condition. These effects were isolated by contrasting event-related activity to the standard (non-target) corner offset stimuli when attended versus unattended. Time-locked ERPs to the standard stimuli were averaged separately according to quadrant of presentation (UL, UR, LL, and LR), and ERPs were re-referenced algebraically to the average of the left and right mastoids. Specifically, the unattended ERPs at a particular location (say, UR) were calculated by averaging over all three of the conditions when the other three quadrants (UL, LL and LR) were attended. This averaging was validated by showing that the ERPs elicited by unattended corner offsets did not differ as a function of which of the other corners was attended ([Martinez et al., 2007](#); Table 3).

Given the similarity of the ERP waveforms across the different quadrants (see [Fig. 2](#)), the present ERP analyses were carried out on waveforms averaged over all quadrants. ERPs to left and right field stimuli were averaged such that electrode sites contralateral to stimulus presentation (in the right and left hemispheres, respectively) were averaged together. Corresponding sites in the ipsilateral hemispheres were similarly averaged together. ERP attention effects were quantified in the waveforms averaged over all quadrants in terms of mean amplitudes within specified latency windows with respect to a 100 ms pre-stimulus baseline. The mean amplitudes of the P1 (88–120 ms) and N1 (148–184 ms) components were subjected to a repeated-measures ANOVA with factors of attention (attended vs. unattended for spatial attention) and hemisphere (ipsilateral vs. contralateral to the eliciting stimulus). In all analyses, P1 and N1 were measured as mean amplitudes averaged over a cluster of 8 posterior electrode sites in each hemisphere (O1/O2, PO3/PO4, PO7/PO8, P3/P4, P5/P6, P7/P8, I3/I4, I5/I6), where these components were largest. The specific time windows used for measuring each component were chosen to encompass the attention-related amplitude modulations that were stable in scalp topography within their respective time windows ([Martinez et al., 2007](#)).

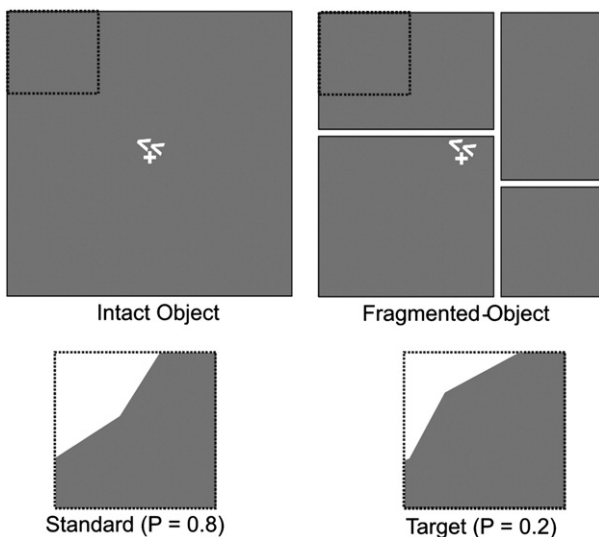


Fig. 1. Stimulus configurations for the intact object (IO) and fragmented object (FO) conditions. In both configurations subjects were cued to covertly attend to one visual quadrant (UL in example shown) and to discriminate brief (100 ms) corner offset stimuli. The offset stimuli left either a concave (standards, $p = 0.8$) or convex (targets, $p = 0.2$) edge. Dotted lines outlining the attended quadrant were not present in the display. The present study was exclusively focused on spatial attention effects in the IO condition.

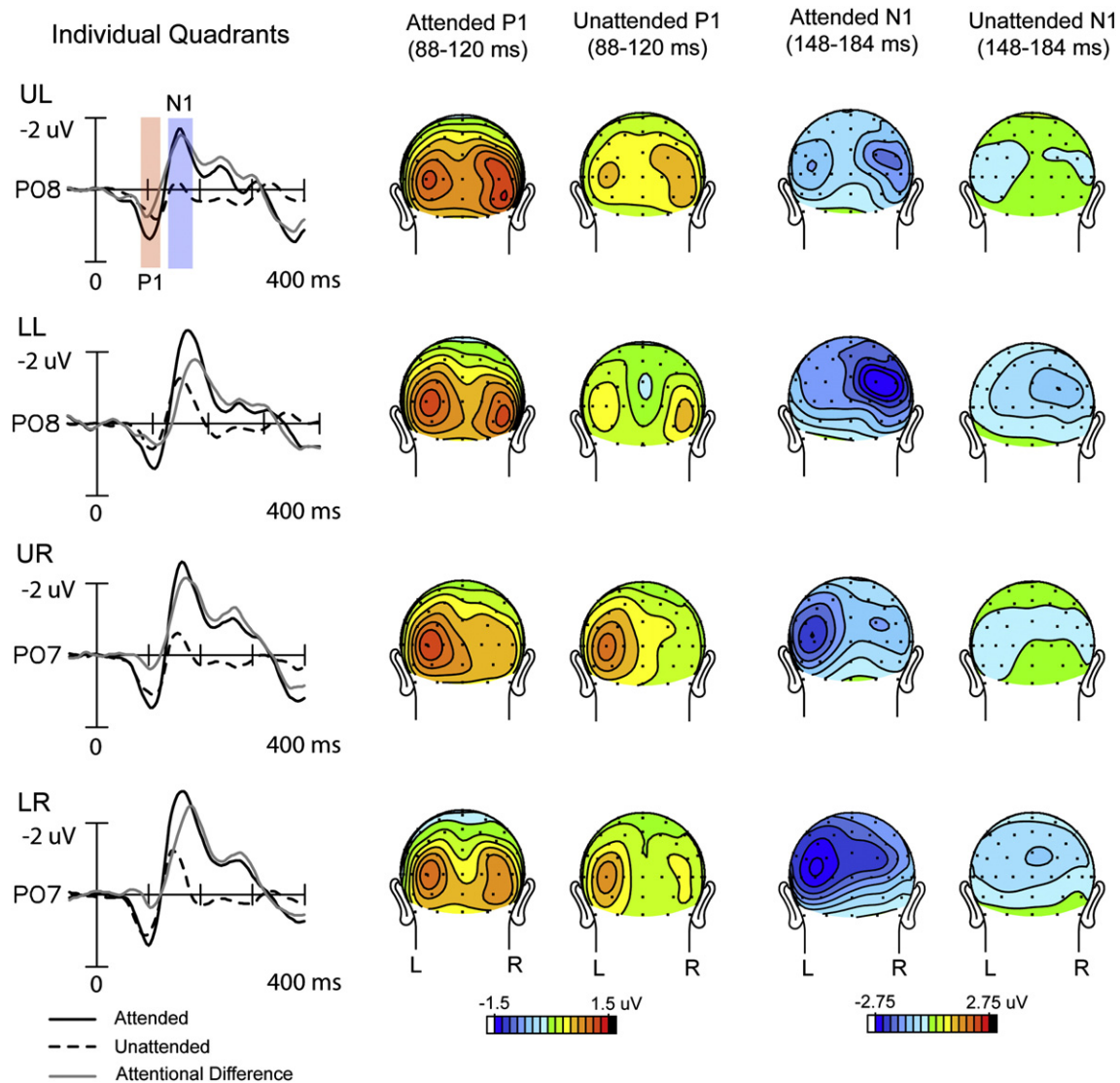


Fig. 2. Grand-averaged ERPs to attended and unattended stimuli and corresponding scalp voltage topographies at P1 (88–120 ms) and N1 (148–184 ms) component latencies within each quadrant (UL: upper left; LL: lower left, UR: upper right, LR: lower right). ERP waveforms are from a parieto-occipital electrode site contralateral to the eliciting stimulus in each quadrant.

Frequency domain analysis

To analyze oscillatory cortical activity following attended and unattended stimuli in each quadrant within the IO conditions, the single trial EEG signal on each channel was convolved with 3-cycle Morlet wavelets computed at each time point (every 4 ms) over a 2 s window centered at stimulus onset. Three-cycle wavelets were chosen as they were found to be optimal for both temporal as well as frequency band resolution. Instantaneous power and phase were extracted at each time point (at 250 Hz sampling rate) over 79 frequency scales from 0.7 to 52.5 Hz incremented logarithmically (Lakatos et al., 2005). Power was calculated as the sum of the squares of the real and imaginary Morlet components. The square roots of the power values, termed spectral amplitudes (in μV), were then averaged over single trials separately for the attended and unattended conditions to yield the total averaged spectral amplitudes for each condition and electrode site. The averaged spectral amplitude at each time point and frequency was baseline corrected by subtracting the mean spectral amplitude over the -300 to -50 ms pre-stimulus interval (corrected separately for each frequency band in each individual subject) (Tallon-Baudry et al., 1998). The phase locking index (PLI) across trials was calculated by normalizing the complex wavelet decomposition

on every trial by its absolute value and averaging this quantity over all trials (Lakatos et al., 2005; Martinez-Montes et al., 2008). The PLI, varying between zero and one, provided a measure of instantaneous spectral phase consistency at each frequency across trials.

In order to analyze the effects of attention in the latency ranges of the attention-related P1 (88–120 ms) and N1 (148–184 ms) ERP components, significant differences in spectral amplitude and phase-locking between the attended and unattended single trial averages were compared in these latency ranges using ANOVA (Kiebel et al., 2005). These analyses were performed in the theta (4–8 Hz) and alpha (8–12 Hz) frequency bands, which were the major constituent frequencies of these ERPs (see below). A caveat of this analysis is that due to the temporal smearing of the three-cycle wavelet transform, single trial neural activity corresponding to the P1 and N1 components cannot be sharply distinguished. Accordingly, we refer to the calculated single trial amplitude and PLI measures as belonging to the P1 and N1 latency ranges rather than to the P1 and N1 components. The fact that very similar attention effects were found in these two latency ranges support our main conclusions about how attention affects neural activity in the P1–N1 range.

Spectral amplitude and PLI measures for each subject were averaged over all quadrants and in addition analyzed for each individual quadrant

(Supplementary Table 1) over the same cluster of 16 posterior electrode sites (8 in each hemisphere) that was used to test the P1/N1 ERP components. Spectral amplitudes and PLIs were first calculated individually for each electrode site and the mean values over each hemisphere were then entered into the ANOVA. The analyses presented here are focused on examining the nature of the attention effects on neural activity (i.e., the attend vs. unattend differences) rather than on the responses to the attended or unattended stimuli by themselves. The attended vs. unattended ANOVA comparisons for PLI were additionally confirmed using a bootstrap ANOVA over 1000 iterations of Monte Carlo resampling (Efron and Tibshirani, 1993; Sprent, 1998).

Wavelet decompositions were also performed on the ERPs averaged over all quadrants in each subject. The spectral amplitudes within the theta and alpha bands were statistically quantified in the P1 and N1 latency ranges using the same ANOVA factors as for the single-trial wavelet decompositions above.

Results

Averaged ERPs analyzed in the time domain

Allocation of spatial attention to one of the four visual quadrant locations resulted in enhanced amplitudes of the early P1 (88–120 ms) and N1 (148–184 ms) components elicited by stimuli at that location (Fig. 2). These effects of spatial attention on the averaged ERP were previously reported by Martinez et al. (2007). Given the similarity of ERP waveforms and attention effects across the four quadrants, ERPs were collapsed to form an average over all quadrants (Fig. 3A), with ERPs averaged separately for the hemispheres contralateral and ipsilateral with respect to stimulus location.

In the ERPs averaged over all quadrants, the amplitudes of the P1 and N1 components were highly significant with respect to the pre-stimulus baseline in both the attended and unattended waveforms (P1: Att: $t(13) = 8.61, p < 0.0001$, Unatt: $t(13) = 5.66, p < 0.0001$, N1: Att: $t(13) = 5.92, p < 0.0001$, Unatt: $t(13) = 2.83, p < 0.02$). Both P1 and N1 components were significantly lateralized to the contralateral hemisphere (Contra vs. Ipsi: P1: $F(1,13) = 5.12, p < 0.05$, N1: $F(1,13) = 9.35, p < 0.01$). The effect of attention on the P1 and N1 components across all quadrants was highly significant (P1: Att vs. unAtt: $F(1,13) = 20.03, p < 0.0007$; N1: Att vs. unAtt: $F(1,13) = 23.26, p < 0.0004$). The N1 attention effect, but not the P1 effect, was significantly larger over contralateral occipital sites as evidenced by the Attention \times Hemisphere (Ipsi vs. Contra.) interaction (P1: $F(1,13) = 1.07, p = n.s.$, N1: $F(1,13) = 22.00, p < 0.0005$).

Averaged ERPs analyzed in the frequency domain

A frequency domain analysis was carried out on the ERPs averaged across all quadrants for each individual subject (the topographies of the grand-averaged time-domain waveforms across all subjects are shown in Fig. 3A). The topographical distributions of the corresponding mean spectral amplitudes of these averaged waveforms in the latency ranges of the P1 and N1 components are illustrated for the dominant theta (Fig. 3B) and alpha (Fig. 3C) frequencies. It is evident that the attended ERPs have considerably larger spectral amplitudes in both the theta and alpha bands than do the unattended ERPs, in both the P1 and N1 latency ranges: (for theta, Att vs. Unatt: P1 range: $F(1,13) = 23.78, p < 0.0004$, N1 range: $F(1,13) = 16.14, p < 0.002$; for alpha, Att vs. Unatt: P1 range: $F(1,13) = 61.26, p < 0.0001$, N1 range: $F(1,13) = 77.93, p < 0.0001$). These spectral amplitudes were larger over the hemisphere contralateral to stimulus presentation for both

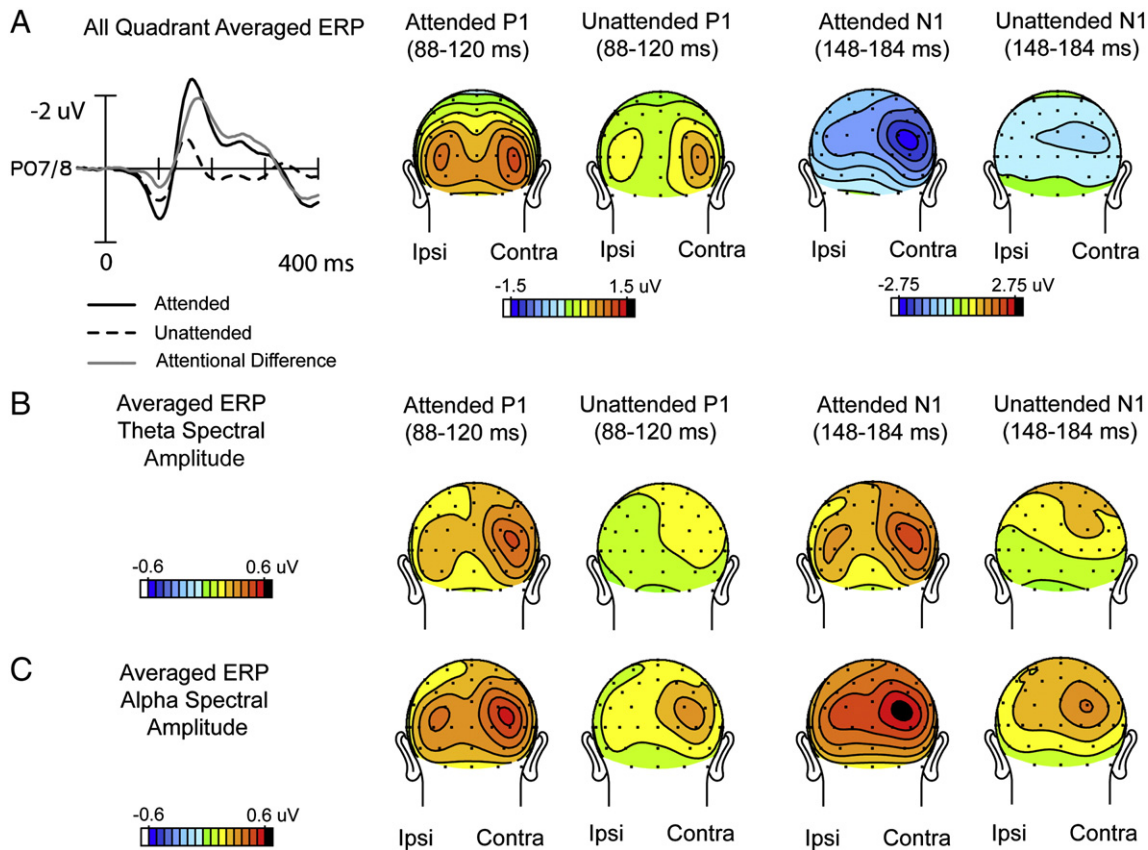


Fig. 3. Grand-averaged ERPs averaged over all quadrants. (A) Time domain waveforms and scalp voltage topographies in the P1 and N1 latency ranges collapsed over left and right quadrants such that contralateral scalp sites are on the right of each head map and ipsilateral sites are on the left. (B) Corresponding topographies of theta spectral amplitudes resulting from wavelet analysis of these ERPs averaged over all quadrants. (C). Same as B for the alpha spectral amplitudes.

the theta (Contra vs. Ipsi: P1 range: $F(1,13)=25.44$, $p<0.0003$, N1 range: $F(1,13)=25.45$, $p<0.0003$) and alpha bands (Contra vs. Ipsi: P1 range: $F(1,13)=12.95$, $p<0.004$, N1 range: $F(1,13)=8.17$, $p<0.02$). Table 1 gives the spectral amplitude values on which these comparisons are based.

Single trials analyzed in the frequency domain

The time-frequency plots resulting from the wavelet decomposition of the single-trial ERPs are shown in Fig. 4. Spectral amplitudes averaged over individual trials and corresponding phase-locking index (PLI) values were averaged over all subjects and over all quadrants. Attention-related modulations of spectral amplitude as well as PLI were evident in the theta (4–8 Hz) and alpha (8–12 Hz) frequency bands within the P1 (88–120 ms) and N1 (148–184 ms) component latencies. The scalp topographies of these spectral amplitude and PLI values were mapped separately for the theta and alpha frequencies within the P1 and N1 time windows. These topographies are shown in comparison with the scalp distributions of the grand-averaged ERP components in Fig. 5.

The single-trial spectral amplitude and PLI modulations depicted in Fig. 5 were quantified at ipsilateral and contralateral occipital sites and averaged over all quadrants (Fig. 6). Within the theta (4–8 Hz) frequency range there was a significant increase in spectral amplitude in the single trial responses to attended versus unattended stimuli in both the P1 and N1 time windows (Att vs. Unatt: P1 range : $F(1,13)=15.97$, $p<0.002$, N1 range : $F(1,13)=16.55$, $p<0.002$). The unattended spectral amplitudes did not significantly differ from baseline in either latency range (Table 1A). Concomitant with the enhanced spectral amplitude, the theta phase consistency as indexed by the PLI was also increased in the attended relative to the unattended single trial responses in both P1 and N1 latency ranges (Att vs. Unatt: P1 range: $F(1,13)=42.45$, $p<0.0001$, N1 range: $F(1,13)=36.20$, $p<0.0001$). As shown in Fig. 5, the topographical distributions of the theta spectral amplitude and the corresponding PLI were very similar, with bilateral maxima over the lateral occipital scalp and a slight contralateral preponderance. These single trial distributions were also similar to the distributions of the spectral amplitude of theta in the averaged ERPs (Fig. 3B). These data provide clear evidence that the attended stimuli elicited additive neural activity with

synaptic currents having a consistent, time-locked waveform in the theta frequency band.

In the alpha (8–12 Hz) frequency band the single trial amplitude modulations showed a similar, though not identical pattern in the P1 and N1 latency ranges. In the P1 range alpha spectral amplitudes to both attended and unattended stimuli were enlarged relative to baseline over both ipsilateral and contralateral sites (Table 1B; Fig. 6B). These spectral amplitudes were significantly larger in response to attended versus unattended stimuli (Att vs. Unatt: $F(1,13)=4.68$, $p<0.05$), but post-hoc analysis showed this alpha increase in the P1 latency range to be significant only over the ipsilateral hemisphere (Att vs. Unatt: ipsi: $F(1,13)=6.66$, $p<0.03$, contra: $F(1,13)=2.35$, $p=n.s.$). Phase consistency, as indexed by the PLI, was significantly increased relative to baseline in the P1 range (Table 1B) and was larger in response to attended versus unattended stimuli over both ipsilateral and contralateral sites (Fig. 6B) (Att vs. Unatt: P1 range: $F(1,13)=36.97$, $p<0.0001$). This pattern of attention effects on the contralateral response (significant increase in PLI without a corresponding increase in spectral amplitude) is consistent with a mechanism of enhanced phase synchronization of the ongoing alpha rhythm by attended stimuli. Over the ipsilateral hemisphere, however, the increased PLI with attention was accompanied by an increase in spectral amplitude, which indicates that the attended stimuli elicited enhanced additive synaptic activity in the alpha frequency band that was phase-locked to the stimulus.

In the N1 latency range the alpha spectral amplitudes exceeded baseline levels only at the ipsilateral hemisphere sites (Table 1B; Fig. 6B). These spectral amplitudes were not affected by spatial attention in either hemisphere (Att. vs. Unatt.: $F(1,13)=0.56$, $p=n.s.$). In contrast, the alpha PLI was significantly increased by attention at both ipsilateral and contralateral sites (Table 1B; Fig. 6B) (Att vs. Unatt: $F(1,13)=26.60$, $p<0.0002$). This pattern of results (increased PLI with no change in spectral amplitude) is also consistent with an attention mechanism that increases alpha phase synchronization, particularly over the contralateral hemisphere. Such a phase synchronization could explain why the contralateral single trial alpha spectral amplitude (relative to baseline) was near zero in the N1 latency range (Fig. 6B), while the alpha spectral amplitude of the averaged ERP (Fig. 3C) shows a large and consistent contralateral dominance.

Table 1
Attended and unattended spectral amplitude and phase locking (PLI) measures (relative to pre-stimulus baseline) at ipsilateral and contralateral occipital sites in the P1 and N1 latency ranges in the (A) theta and (B) alpha frequency bands. Averaged ERP spectral amplitudes were obtained from wavelet decompositions of the all-quadrant-averaged ERPs. Associated t-tests indicate significance levels with respect to baseline.

| | | Hemi | Spectral amplitude (μV) | | | | | | Phase locking index (PLI) | | | | | |
|--------------------|--------------|--------|--------------------------------|-------|--------|-------|-------|--------|---------------------------|-------|--------|--------|-------|--------|
| | | | Att. | t(13) | p< | Unatt | t(13) | p< | Att. | t(13) | p< | Unatt. | t(13) | p< |
| A) Theta (4–8 Hz) | | | | | | | | | | | | | | |
| P1 latency | Single-trial | Ipsi | 0.20 | 3.61 | 0.004 | –0.05 | 1.80 | n.s. | 0.22 | 8.44 | 0.0001 | 0.08 | 9.19 | 0.0001 |
| | | Contra | 0.24 | 5.82 | 0.0001 | –0.01 | 0.48 | n.s. | 0.26 | 10.42 | 0.0001 | 0.14 | 9.32 | 0.0001 |
| | Averaged ERP | Ipsi | 0.33 | 5.33 | 0.0002 | 0.12 | 9.11 | 0.0001 | | | | | | |
| | | Contra | 0.47 | 7.75 | 0.0001 | 0.22 | 7.82 | 0.0001 | | | | | | |
| N1 latency | Single-trial | Ipsi | 0.27 | 4.45 | 0.0007 | –0.05 | 1.35 | n.s. | 0.23 | 8.45 | 0.0001 | 0.09 | 8.41 | 0.0001 |
| | | Contra | 0.31 | 4.91 | 0.0003 | –0.02 | 1.05 | n.s. | 0.27 | 10.44 | 0.0001 | 0.15 | 10.90 | 0.0001 |
| | Averaged ERP | Ipsi | 0.37 | 4.91 | 0.0003 | 0.15 | 8.28 | 0.0001 | | | | | | |
| | | Contra | 0.51 | 6.74 | 0.0001 | 0.25 | 7.89 | 0.0001 | | | | | | |
| B) Alpha (8–12 Hz) | | | | | | | | | | | | | | |
| P1 latency | Single-trial | Ipsi | 0.24 | 8.07 | 0.0001 | 0.13 | 2.52 | 0.03 | 0.19 | 8.27 | 0.0001 | 0.09 | 7.07 | 0.0001 |
| | | Contra | 0.15 | 3.92 | 0.002 | 0.08 | 2.22 | 0.05 | 0.20 | 8.29 | 0.0001 | 0.11 | 6.28 | 0.0001 |
| | Averaged ERP | Ipsi | 0.38 | 11.24 | 0.0001 | 0.18 | 9.00 | 0.0001 | | | | | | |
| | | Contra | 0.47 | 13.85 | 0.0001 | 0.27 | 8.85 | 0.0001 | | | | | | |
| N1 latency | Single-trial | Ipsi | 0.20 | 4.59 | 0.0006 | 0.16 | 2.87 | 0.02 | 0.17 | 8.83 | 0.0001 | 0.10 | 6.28 | 0.0001 |
| | | Contra | 0.02 | 0.39 | n.s. | –0.04 | –0.86 | n.s. | 0.19 | 9.13 | 0.0001 | 0.11 | 7.46 | 0.0001 |
| | Averaged ERP | Ipsi | 0.47 | 12.92 | 0.0001 | 0.24 | 9.13 | 0.0001 | | | | | | |
| | | Contra | 0.55 | 13.28 | 0.0001 | 0.31 | 8.99 | 0.0001 | | | | | | |

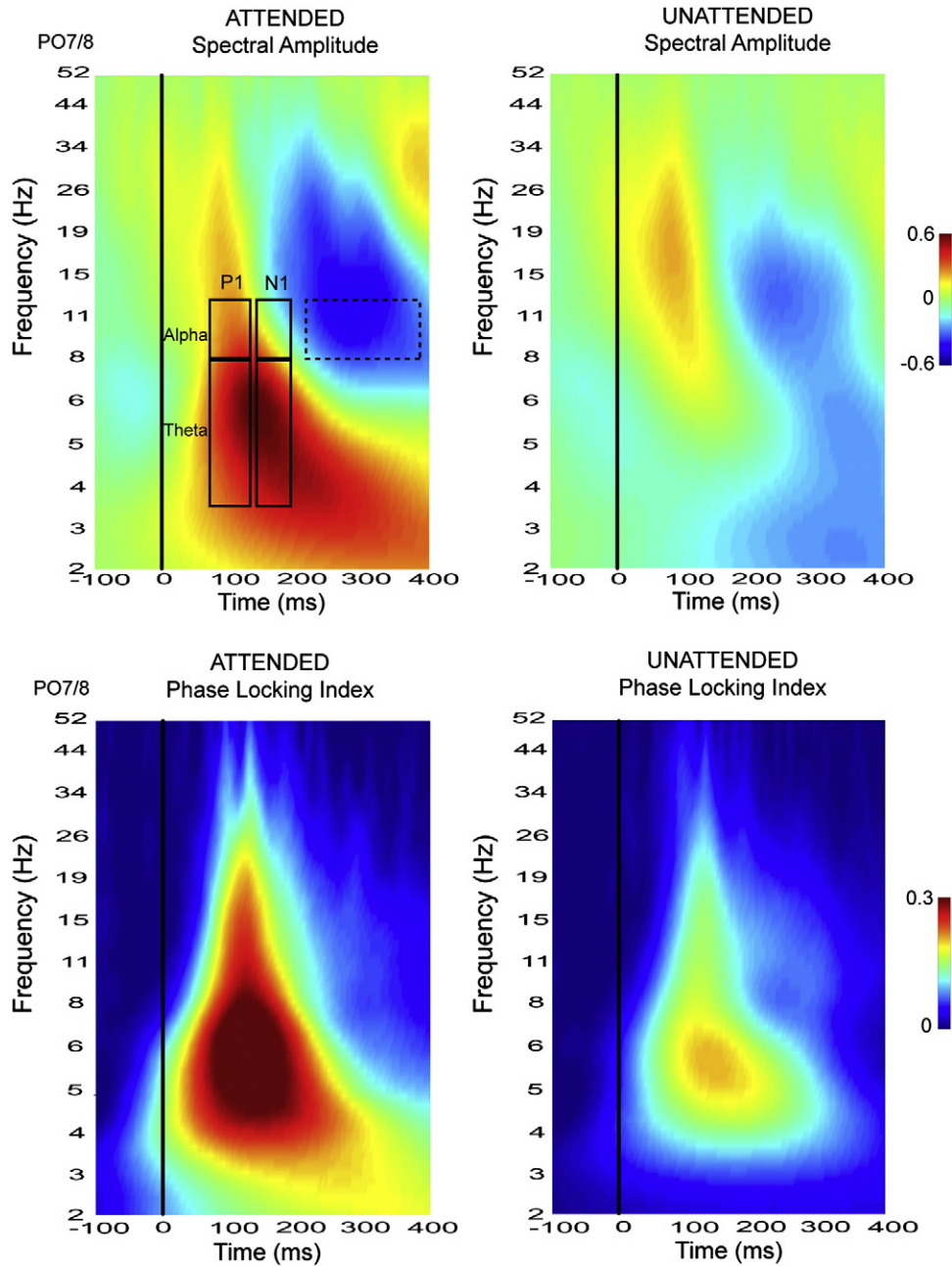


Fig. 4. Time-frequency plots of spectral amplitude and phase locking index (PLI) measures derived from the frequency domain wavelet decomposition of single-trial ERPs. Plots shown were based on ERPs recorded from a contralateral parieto-occipital site, averaged over single trials and grand averaged over all subjects and over all quadrants. Single-trial modulations were quantified within theta (4–8 Hz) and alpha (8–12 Hz) frequency bands in the P1 and N1 latency ranges as outlined in the top-left spectral image. The latency range over which alpha suppression was measured (215–375 ms) is demarcated by a dashed rectangle.

Each of the above-mentioned attention effects on PLI was confirmed by bootstrap ANOVAs over 1000 Monte Carlo iterations and found to be significant (P1 latency range: theta: $F=26.17$, $p<0.0001$, alpha: $F=11.92$, $p<0.002$; N1 latency range: theta: $F=22.53$, $p<0.0001$, alpha: $F=10.95$, $p<0.005$). The attentional modulations of spectral amplitude and PLI characterized above in the single trial ERPs averaged over all quadrants, were also found to be consistently present within individual quadrants (Supplementary Table 1).

Interactions with ongoing pre-stimulus EEG activity

The foregoing analyses demonstrated that the modulations of P1/N1 amplitudes with attention included the triggering of additive neural activity in the theta band, whereas in the alpha band the

finding of increased phase locking in the absence of increased single trial spectral amplitude suggested an attention mechanism of increased phase synchronization of the ongoing alpha activity. There is an alternative mechanism, however, that could account for the alpha band attention effects. If the attended stimuli provoked a greater blocking or suppression of the ongoing alpha rhythm than did the unattended stimuli (e.g., Mazaheri and Picton, 2005; Min et al., 2007; Siegel et al., 2008; Vanni et al., 1997; Yamagishi et al., 2003), this reduction in alpha would tend to cancel out any concurrent increase in alpha amplitude that may have been produced by an increased additive neural response. To evaluate this possibility we examined correlations between the pre-stimulus (baseline) alpha activity in the EEG prior to stimulus presentations and the modulations of the post-stimulus EEG/ERP produced by attention. Using model simulations

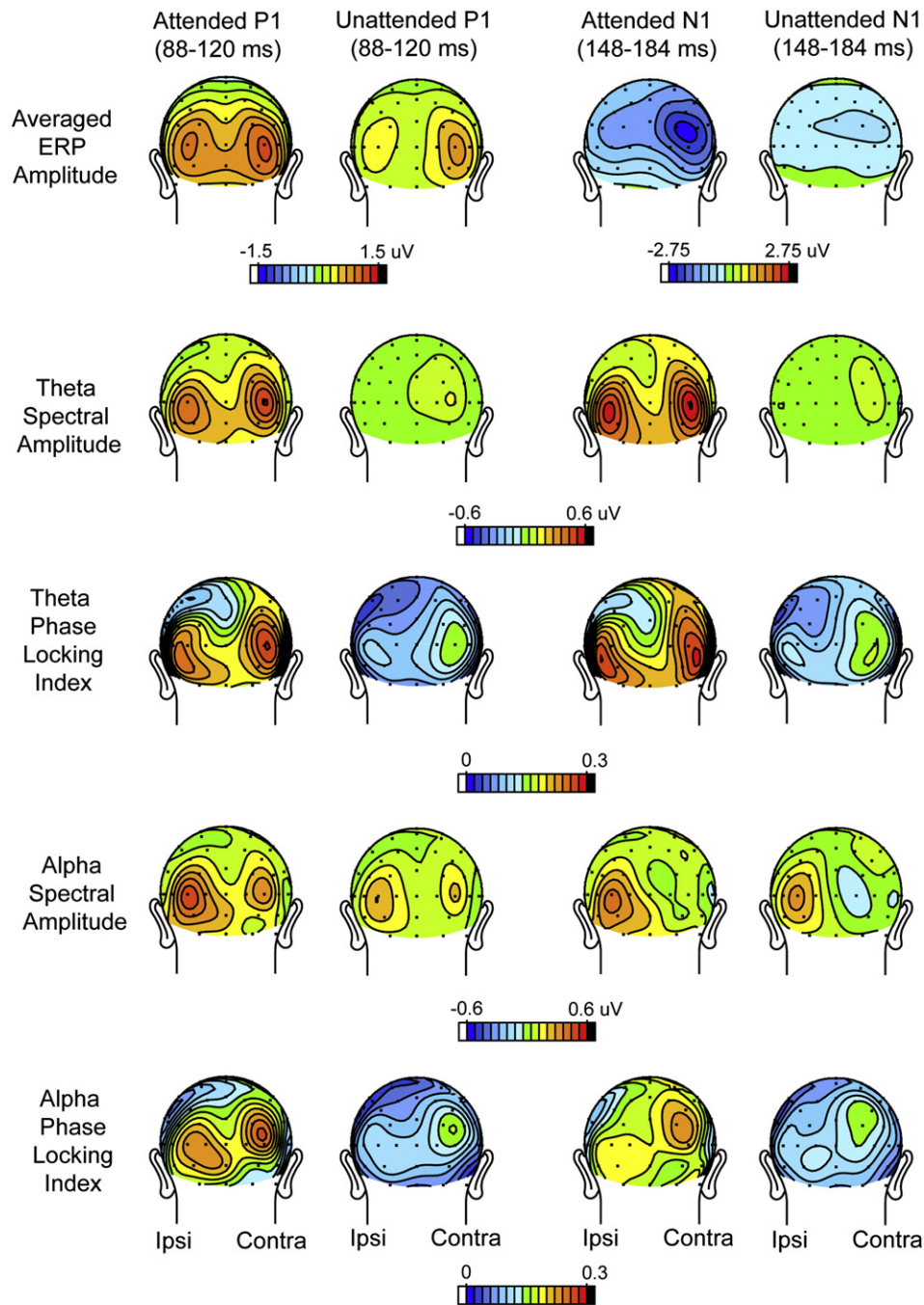


Fig. 5. Scalp topographies of the single-trial spectral amplitudes and PLI values in the theta and alpha frequency bands within the P1 and N1 latency ranges. To obtain these maps the single trial values were averaged over all quadrants and all subjects. The first row (same as Fig. 2A) shows grand-averaged voltage distributions of the ERP components for comparison.

as well as experimental data, Min et al. (2007) and Becker et al. (2008) have shown how such correlations can help to distinguish between the “additive-response” and “phase-reset” mechanisms. In particular, these authors proposed that higher baseline levels of pre-stimulus alpha activity would be correlated with a greater post-stimulus desynchronization (blocking) relative to baseline that would tend to cancel out any stimulus-evoked additive activity. Moreover, higher levels of pre-stimulus alpha should be correlated with larger amplitudes of averaged ERPs if those ERPs were produced by phase synchronization of the ongoing alpha, but no such correlation should be found if the ERPs resulted from stimulus-elicited neural activity that was additive with the ongoing EEG. In order to study these correlations, we quantified the baseline alpha levels and the post-stimulus alpha blocking as described below.

Baseline spectral EEG amplitudes were calculated from the wavelet analysis over the interval -300 to -48 ms prior to each stimulus over the same cluster of 16 posterior electrode sites (8 in each hemisphere) that was used to measure the P1/N1 amplitudes. Ongoing theta and alpha rhythms had significant spectral amplitudes in this baseline window preceding both attended and unattended stimuli (theta: Att: $2.97 \pm 0.31 \mu\text{V}$ ($t(13) = 9.70$, $p < 0.0001$), Unatt: $2.97 \pm 0.30 \mu\text{V}$ ($t(13) = 9.85$, $p < 0.0001$); alpha: Att: $4.39 \pm 0.56 \mu\text{V}$ ($t(13) = 7.80$, $p < 0.0001$), Unatt: $4.36 \pm 0.56 \mu\text{V}$ ($t(13) = 7.91$, $p < 0.0001$)). As would be expected given the randomized order of stimulus presentation, there was no significant difference between the attended and unattended baseline amplitudes in either the theta ($F(1,13) = 0.09$, $p = n.s.$) or alpha ($F(1,13) = 2.12$, $p = n.s.$) frequency bands. Nor did the amplitudes of these pre-stimulus EEG

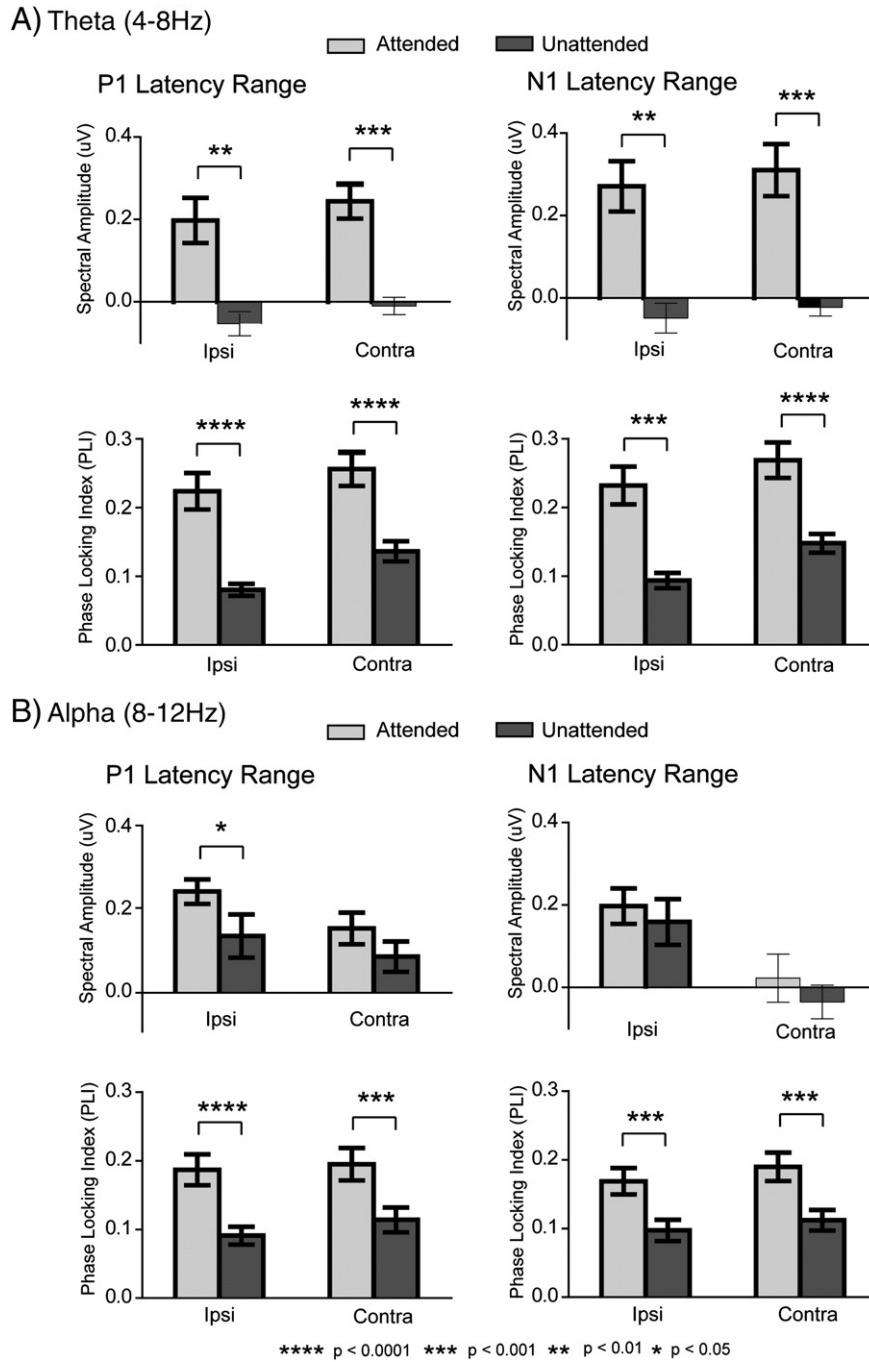


Fig. 6. Spectral amplitudes and PLI values for attended and unattended single-trial responses at ipsilateral and contralateral occipital sites within (A) theta and (B) alpha frequency bands within the P1 (left column) and N1 (right column) latency ranges. Data are averaged over all quadrants and all subjects.

rhythms differ significantly between the hemispheres contralateral and ipsilateral to the attended visual field (theta: $F(1,13) = 0.14$, $p = n.s.$, alpha: $F(1,13) = 2.40$, $p = n.s.$).

To obtain a measure of alpha blocking (suppression) following each stimulus, the mean alpha band spectral amplitude was calculated relative to the above-mentioned baseline over the 215–375 ms post-stimulus interval (i.e., immediately following the N1 component), where a strong alpha suppression was evident (see dashed outlined box in Fig. 4). This alpha suppression was maximal over occipital sites contralateral to the side of stimulus presentation (contra vs. ipsi, $F(1,13) = 11.61$, $p < 0.005$) (Fig. 7), and this contralateral suppression was considerably larger following attended ($-0.24 \pm 0.15 \mu V$) than unattended ($-0.14 \pm 0.04 \mu V$) stimuli. Due to the large inter-subject variability of the alpha suppression following attended stimuli,

however, this contralateral attention effect did not reach significance ($F(1,13) = 0.42$, $p = n.s.$). Nonetheless, subjects who showed relatively greater contralateral alpha suppression following attended (versus unattended) stimuli were found to have a reduced increment in single trial alpha power with attention in both the P1 ($r(12) = 0.80$, $p < 0.0006$) and N1 ($r(12) = 0.82$, $p < 0.0004$) latency ranges. These between-subject correlations are in line with the hypothesis that post-stimulus alpha blocking was counteracting the increased spectral amplitude in the P1 and N1 latency ranges following attended stimuli, resulting in little or no net change in spectral amplitude. Consistent with this hypothesis were significant *negative* between-subject correlations between the amplitude of the pre-stimulus contralateral baseline alpha and the magnitude of the single trial attentional modulation (attended minus unattended) of alpha spectral amplitude in both the P1 ($r(12) =$

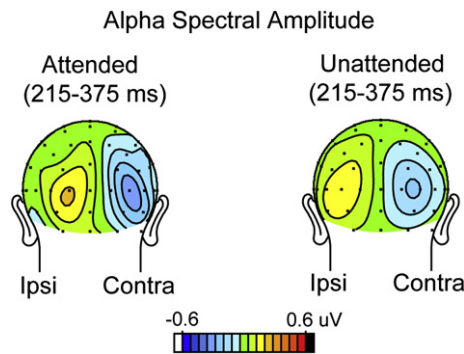


Fig. 7. Scalp topography of the suppression (blocking) of the ongoing alpha rhythm following attended (left) and unattended (right) stimuli. Alpha suppression was calculated from the wavelet analysis over the interval 215–375 ms with respect to the pre-stimulus baseline alpha level. This suppression was much larger over the occipital scalp contralateral to the stimulus (right side of each head) than over the ipsilateral scalp (left side of each head).

–0.91, $p < 0.0001$) and N1 ($r(12) = -0.77$, $p < 0.002$) latency ranges. This result is congruent with the predictions of the “additive-response” model as analyzed by Becker et al. (2008), who postulated that subjects with higher levels of baseline alpha would exhibit a larger stimulus-induced alpha blocking. In the present experiment such blocking would tend to cancel out any additive neural activity that was elicited by attended stimuli.

A third finding that weighs against increased phase synchronization as the sole mechanism of attentional modulation in the alpha band was the absence of any significant positive correlations between the contralateral baseline alpha level and the amplitude of the attentional modulation (attended minus unattended) of the averaged ERPs in the time domain. Following the analysis of Becker et al. (2008), if the effects of attention on the averaged ERPs were produced by increased phase synchronization of the EEG following attended stimuli, these attention effects should be larger when baseline alpha levels are larger. In fact, the correlations between contralateral baseline alpha amplitude and ERP amplitudes were negative for both the P1 ($r(12) = -0.58$, $p < 0.03$) and N1 ($r(12) = -0.40$, $p = 0.1$) component, suggesting that higher pre-stimulus alpha actually led to smaller attentional modulations.

A fourth line of evidence that the ERP modulations in this study were not produced solely by phase synchronization of the ongoing alpha rhythm comes from findings of significant and near-significant inverse correlations between baseline alpha amplitude and the PLI (baseline alpha amplitude vs. attended alpha PLI: P1 latency: $r(12) = -0.69$, $p < 0.007$; N1 latency: $r(12) = -0.45$, $p < 0.06$). As Becker et al. (2008) previously showed, the PLI should not vary as a function of baseline alpha level with a pure phase reset mechanism but would vary inversely with alpha level in an additive “evoked model”, because the fixed-phase evoked response would become relatively smaller as the amplitude of the baseline alpha rhythm increased.

Discussion

The present study used time- and frequency-domain analyses to investigate the neural mechanisms of generation of early ERP components that were enhanced by the allocation of spatial attention. These ERPs were recorded in a previous study (Martinez et al., 2007), which found that amplitudes of the early P1 (88–120 ms) and N1 (148–184 ms) components of the visual ERP were markedly enlarged to stimuli at attended locations in the visual field. By making wavelet decompositions of the single trial EEG epochs from the Martinez et al. (2007) study, we found that the enhanced ERP amplitudes observed in the time domain were associated with an increase of

additive, phase-locked theta (4–8 Hz) power in the P1–N1 latency range in response to stimuli at attended locations. The scalp topographies of this increased theta power and phase-locking in the P1–N1 latency range had a maximal amplitude over the lateral occipital scalp that corresponded closely with the topographies of the P1 and N1 components that were enhanced by attention in the time-domain waveforms. This analysis supports the conclusion that the attention-related increase of P1–N1 amplitudes in the averaged ERP may be attributed to an additive increase in the time-locked neural activity in the theta band triggered by the attended stimuli. While it is well-documented in animal studies (see below) that stimuli at attended locations elicit enhanced short-latency neural discharge in the extrastriate visual cortex, the present analysis to our knowledge provides the most direct evidence to date for such an increase in humans.

The present EEG/ERP findings are consistent with the results of many neurophysiological studies in non-human primates, which have shown that spatial attention produces increased firing rates (i.e., additional evoked activity) in neural populations within multiple extrastriate visual cortical areas (e.g., Lee et al., 2007; Luck et al., 1997; Maunsell and McAdams, 2000; Reynolds, 2004; Reynolds and Desimone, 2003). Homologous extrastriate brain regions have been identified as the neural sources of the P1 and N1 ERP components in humans using inverse source modeling procedures (e.g., Di Russo et al., 2002, 2003, 2011; Martinez et al., 1999, 2006, 2007; Vanni et al., 2004). The present results are also consistent with the hypothesis that spatial attention boosts the sensory gain or amplification of attended inputs at the level of the extrastriate visual cortex (Hillyard et al., 1998) and are further compatible with time-frequency analyses of human magneto-encephalographic (MEG) recordings (Mazaheri and Jensen, 2006), which found evoked theta activity to underlie the attended response to a lateralized visual stimulus.

The mechanisms of generation of the visual ERP have been much debated in the recent literature. Some studies have concluded that the averaged ERP emerges as the result of stimulus induced phase-resetting of ongoing oscillatory rhythms (Basar et al., 1980; Brandt et al., 1991; Gruber et al., 2005; Hanslmayr et al., 2007; Jansen et al., 2003; Klimesch et al., 2004; Klimesch et al., 2007a,c; Makeig et al., 2002), while others have supported the view that new stimulus-evoked neural activity is added to the spontaneously ongoing oscillations (Becker et al., 2008; Fell et al., 2004; Mäkinen et al., 2005; Mazaheri and Jensen, 2006; Shah et al., 2004). As both phase synchronization of ongoing oscillations and the addition of time-locked neural activity would increase post-stimulus phase consistency, it is not always easy to discriminate which of these is the primary mechanism of ERP generation (Sauseng et al., 2007; Yeung et al., 2004). Shah et al. (2004) proposed three explicit criteria to distinguish between the phase-reset and evoked models of ERP generation. For the phase-reset model to hold true: (i) EEG oscillations must be significantly present prior to stimulus onset, (ii) stimulus induced phase concentration must occur, and (iii) such phase concentration must not be accompanied by a stimulus induced increase in signal power. On the other hand, to establish an added-activity mechanism criterion (i) is not essential and phase consistency as per criterion (ii) may be present, but most importantly, (iii) stimulus-induced increase in signal power must occur. In the present study we applied these criteria to measures of single-trial event-related EEG activity in the theta and alpha bands, which were the dominant frequencies of the P1 and N1 components that were modulated by spatial attention. As discussed above, the attention-related theta modulations clearly fit the criteria for a mechanism of additive neural activity. The attention-related modulations of the alpha band EEG, however, were not so straightforward, as discussed below.

In the single-trial EEG epochs there was stimulus-induced phase-locking (increased PLI) in the alpha band that was significantly enhanced following attended versus unattended stimuli in both the P1 and N1 latency ranges. Attended single-trial spectral amplitudes,

however, were only weakly enhanced in the P1 latency range, primarily over ipsilateral occipital sites and were not enhanced at all in the N1 latency range. In contrast with this absence of significant enhancement of single-trial alpha amplitudes, the amplitudes of the P1–N1 components in the averaged time-domain ERPs were substantially increased by attention. These findings would appear to fit the criteria for a phase-reset mechanism of attention in the alpha band, which produces a P1–N1 amplitude increase in the averaged time-domain waveforms, in conjunction with a small increment of new additive activity at ipsilateral hemispheric sites.

It has been pointed out, however, that a finding of increased phase synchronization in the absence of increased single-trial spectral amplitude does not provide unequivocal evidence for a phase-resetting mechanism. An alternative scenario for such a data pattern would be that new, phase-locked neural activity is triggered by the stimulus, but this is counteracted by a concurrent suppression or blocking of the ongoing EEG rhythm in the same frequency band (Becker et al., 2008; Hanslmayr et al., 2007; Klimesch et al., 2004; Martinez-Montes et al., 2008; Min et al., 2007). Indeed, many studies have shown that task-relevant visual stimuli can suppress ongoing alpha oscillations (Gruber et al., 2005; Kaufman et al., 1990; Mazaheri and Jensen, 2006; Mazaheri and Picton, 2005; Min et al., 2007; Siegel et al., 2008; Vanni et al., 1997; Yamagishi et al., 2003). There is also evidence to show that alpha is actively enhanced at cortical sites processing irrelevant distracter information in attention tasks (Händel et al., 2011; Kelly et al., 2006; Rihs et al., 2007). It has been inferred from such observations that ongoing alpha oscillations inhibit stimulus processing, and that visual stimulation releases this inhibition by suppressing spontaneous alpha (Klimesch et al., 2007b).

In the present study four separate lines of evidence suggested that the effects of attention on single trial spectral amplitude measures in the alpha band were strongly impacted by a concurrent blocking (suppression) of the ongoing, pre-stimulus alpha EEG. First, in subjects who showed a greater degree of post-stimulus blocking of the pre-stimulus baseline alpha rhythm, there was a reduction in the attention-related enhancement of the single trial spectral amplitudes in the P1/N1 range. Second, these single-trial spectral amplitudes also correlated inversely between subjects with the amplitude of the pre-stimulus alpha rhythm, consistent with the proposition that higher levels of baseline alpha would enable a greater degree of stimulus-induced alpha blocking (Becker et al., 2008; Min et al., 2007). Third, the amplitude of the pre-stimulus alpha EEG did not correlate positively with the attention-related increase in P1 or N1 amplitude in the time-domain averaged ERP (the correlations were actually negative). Such a positive correlation would be expected if the amplitude increases of the time-domain ERP with attention had been produced by a phase synchronization of the ongoing alpha rhythm (Becker et al., 2008). Finally, the amplitude of the pre-stimulus baseline alpha was found to correlate negatively with the degree of alpha phase locking (PLI) in the 80–200 ms range; such a negative correlation is more consistent with an additive-evoked mechanism than with a phase-reset mechanism (Becker et al., 2008). In light of this correlational evidence, it seems most likely that the attended stimuli did in fact elicit enhanced additive, phase-locked neural activity in the alpha band, which was counteracted by a concurrent suppression of the ongoing alpha rhythm in the single-trial spectral amplitude measures. The possibility that partial phase-synchronization of the ongoing alpha rhythm might also have occurred and contributed to the attention effects on the early ERP components cannot be ruled out, however.

In summary, the present results provide insight into the neural mechanisms responsible for the modulation of early ERP components by spatial attention. While the respective roles played by EEG phase resetting and additive neural activity in the generation of ERPs have been debated extensively, the present study is the first to our knowledge to investigate how these alternative mechanisms come into play during selective attention in humans. The present single-trial spectral analyses

revealed that the enhanced amplitudes of the P1 and N1 components of the averaged ERP to attended stimuli can be attributed in large measure to the triggering of additive synaptic activity time-locked to the stimulus with a consistent waveform in the theta frequency band. Attention-related modulations in the alpha band proved more difficult to characterize. Correlations between pre- and post-stimulus alpha activity strongly suggested that attended stimuli elicited new additive neural activity that was masked by the blocking of the ongoing alpha EEG, but a possible contribution of increased phase synchronization of the ongoing alpha rhythm could not be excluded. Indeed, increases in both stimulus-evoked neural activity and phase synchronization would be expected to enhance the strength of the neural representations of attended stimuli in the visual cortex (Salinas and Sejnowski, 2001; Schroeder and Lakatos, 2009; Womelsdorf and Fries, 2007).

Supplementary materials related to this article can be found online at [doi:10.1016/j.neuroimage.2011.09.028](https://doi.org/10.1016/j.neuroimage.2011.09.028).

Acknowledgments

This work was supported by grants from NIMH (R24MH082790 and P50MH86385), NSF (BCS-1029084) and ONR (N00014-07-I-0997). We thank Peter Lakatos for his technical advice.

References

- Basar, E., Gonder, A., Ungan, P., 1980. Comparative frequency analysis of single EEG-evoked potential records. *J. Biomed. Eng.* 2, 9–14.
- Becker, R., Ritter, P., Villringer, A., 2008. Influence of ongoing alpha rhythm on the visual evoked potential. *NeuroImage* 39, 707–716.
- Brandt, M.E., Jansen, B.H., Carbonari, J.P., 1991. Pre-stimulus spectral EEG patterns and the visual evoked response. *Electroencephalogr. Clin. Neurophysiol.* 80, 16–20.
- Di Russo, F., Stella, A., Spitoni, G., Strappini, F., Sdoia, S., Galati, G., Hillyard, S., Spinelli, D., Pitzalis, S., 2011. Spatio-temporal brain mapping of spatial attention effects on pattern-reversal ERPs. *Hum. Brain Mapp.* doi:10.1002/hbm.21285
- Di Russo, F., Martínez, A., Hillyard, S.A., 2003. Source analysis of event-related cortical activity during visuo-spatial attention. *Cerebral cortex (New York, N.Y. : 1991)* 13, 486–499.
- Di Russo, F., Martínez, A., Sereno, M.I., Pitzalis, S., Hillyard, S.A., 2002. Cortical sources of the early components of the visual evoked potential. *Hum. Brain Mapp.* 15, 95–111.
- Efron, B., Tibshirani, R.J., 1993. *An Introduction to the Bootstrap*. Chapman & Hall, London.
- Fell, J., Dietl, T., Grunwald, T., Kurthen, M., Klaver, P., Trautner, P., Schaller, C., Elger, C.E., Fernandez, G., 2004. Neural bases of cognitive ERPs: more than phase reset. *J. Cogn. Neurosci.* 16, 1595–1604.
- Gruber, W.R., Klimesch, W., Sauseng, P., Doppelmayr, M., 2005. Alpha phase synchronization predicts P1 and N1 latency and amplitude size. *Cereb. Cortex* 15, 371–377.
- Händel, B.F., Haarmeier, T., Jensen, O., 2011. Alpha oscillations correlate with the successful inhibition of unattended stimuli. *J. Cogn. Neurosci.* 23, 2494–2502.
- Hanslmayr, S., Klimesch, W., Sauseng, P., Gruber, W., Doppelmayr, M., Freunberger, R., Pecherstorfer, T., Birbaumer, N., 2007. Alpha phase reset contributes to the generation of ERPs. *Cereb. Cortex* 17, 1–8.
- Hillyard, S.A., Anillo-Vento, L., 1998. Event-related brain potentials in the study of visual selective attention. *Proc. Natl. Acad. Sci. U. S. A.* 95, 781–787.
- Hillyard, S.A., Vogel, E.K., Luck, S.J., 1998. Sensory gain control (amplification) as a mechanism of selective attention: electrophysiological and neuroimaging evidence. *Philos. Trans. R. Soc. Lond. B Biol. Sci.* 353, 1257–1270.
- Hopf, J.-M., Heinze, H.-J., Schoenfeld, M.A., Hillyard, S.A., 2009. Spatiotemporal analysis of visual attention. In: In: Gazzaniga, M.S. (Ed.), *The Cognitive Neurosciences*. MIT Press, pp. 235–250.
- Jansen, B.H., Agarwal, G., Hegde, A., Boutros, N.N., 2003. Phase synchronization of the ongoing EEG and auditory EP generation. *Clin. Neurophysiol.* 114, 79–85.
- Kaufman, L., Schwartz, B., Salustri, C., Williamson, S.J., 1990. Modulation of spontaneous brain activity during mental imagery. *J. Cogn. Neurosci.* 2, 124–132.
- Kelly, S.P., Lalor, E.C., Reilly, R.B., Foxe, J.J., 2006. Increases in alpha oscillatory power reflect an active retinotopic mechanism for distracter suppression during sustained visuospatial attention. *J. Neurophysiol.* 95, 3844–3851.
- Kiebel, S.J., Tallon-Baudry, C., Friston, K.J., 2005. Parametric analysis of oscillatory activity as measured with EEG/MEG. *Hum. Brain Mapp.* 26, 170–177.
- Klimesch, W., Hanslmayr, S., Sauseng, P., Gruber, W.R., Doppelmayr, M., 2007a. P1 and traveling alpha waves: evidence for evoked oscillations. *J. Neurophysiol.* 97, 1311–1318.
- Klimesch, W., Sauseng, P., Hanslmayr, S., 2007b. EEG alpha oscillations: the inhibition-timing hypothesis. *Brain Res. Rev.* 53, 63–88.
- Klimesch, W., Sauseng, P., Hanslmayr, S., Gruber, W., Freunberger, R., 2007c. Event-related phase reorganization may explain evoked neural dynamics. *Neurosci. Biobehav. Rev.* 31, 1003–1016.

- Klimesch, W., Schack, B., Schabus, M., Doppelmayr, M., Gruber, W., Sauseng, P., 2004. Phase-locked alpha and theta oscillations generate the P1–N1 complex and are related to memory performance. *Brain Res. Cogn. Brain Res.* 19, 302–316.
- Lakatos, P., Shah, A.S., Knuth, K.H., Ulbert, I., Karmos, G., Schroeder, C.E., 2005. An oscillatory hierarchy controlling neuronal excitability and stimulus processing in the auditory cortex. *J. Neurophysiol.* 94, 1904–1911.
- Lee, J., Williford, T., Maunsell, J.H., 2007. Spatial attention and the latency of neuronal responses in macaque area V4. *J. Neurosci.* 27, 9632–9637.
- Luck, S.J., Girelli, M., McDermott, M.T., Ford, M.A., 1997. Bridging the gap between monkey neurophysiology and human perception: an ambiguity resolution theory of visual selective attention. *Cogn. Psychol.* 33, 64–87.
- Makeig, S., Westerfield, M., Jung, T.P., Enghoff, S., Townsend, J., Courchesne, E., Sejnowski, T.J., 2002. Dynamic brain sources of visual evoked responses. *Science* 295, 690–694.
- Makinen, V., Tiitinen, H., May, P., 2005. Auditory event-related responses are generated independently of ongoing brain activity. *Neuroimage* 24, 961–968.
- Martinez, A., et al., 1999. Involvement of striate and extrastriate visual cortical areas in spatial attention. *Nat. Neurosci.* 2, 364–369.
- Martinez, A., Ramanathan, D.S., Foxe, J.J., Javitt, D.C., Hillyard, S.A., 2007. The role of spatial attention in the selection of real and illusory objects. *J. Neurosci.* 27, 7963–7973.
- Martinez, A., Teder-Salejarvi, W., Vazquez, M., Molholm, S., Foxe, J.J., Javitt, D.C., Di Russo, F., Worden, M.S., Hillyard, S.A., 2006. Objects are highlighted by spatial attention. *J. Cogn. Neurosci.* 18, 298–310.
- Martinez-Montes, E., Cuspineda-Bravo, E.R., El-Deredy, W., Sanchez-Bornot, J.M., Lage-Castellanos, A., Valdes-Sosa, P.A., 2008. Exploring event-related brain dynamics with tests on complex valued time-frequency representations. *Stat. Med.* 27, 2922–2947.
- Maunsell, J.H., McAdams, C.J., 2000. In: Gazzaniga, M.S. (Ed.), *Effects of Attention on Neuronal Response Properties in Visual Cerebral Cortex*. M.I.T. Press, Cambridge, MA, pp. 290–305.
- Mazaheri, A., Jensen, O., 2006. Posterior alpha activity is not phase-reset by visual stimuli. *Proc. Natl. Acad. Sci. U. S. A.* 103, 2948–2952.
- Mazaheri, A., Picton, T.W., 2005. EEG spectral dynamics during discrimination of auditory and visual targets. *Brain Res. Cogn. Brain Res.* 24, 81–96.
- Min, B.K., Busch, N.A., Debener, S., Kranczioch, C., Hanslmayr, S., Engel, A.K., Herrmann, C.S., 2007. The best of both worlds: phase-reset of human EEG alpha activity and additive power contribute to ERP generation. *Int. J. Psychophysiol.* 65, 58–68.
- Noesselt, T., Hillyard, S.A., Woldorff, M.G., Schoenfeld, A., Hagner, T., Jancke, L., Tempelmann, C., Hinrichs, H., Heinze, H.J., 2002. Delayed striate cortical activation during spatial attention. *Neuron* 35, 575–587.
- Reynolds, J.H., 2004. In: Posner, M.I. (Ed.), *Attention and Contrast Gain Control*. Guilford Press, pp. 127–143.
- Reynolds, J.H., Desimone, R., 2003. Interacting roles of attention and visual salience in V4. *Neuron* 37, 853–863.
- Rihs, T.A., Michel, C.M., Thut, G., 2007. Mechanisms of selective inhibition in visual spatial attention are indexed by alpha-band EEG synchronization. *Eur. J. Neurosci.* 25, 603–610.
- Salinas, E., Sejnowski, T.J., 2001. Correlated neuronal activity and the flow of neural information. *Nat. Rev. Neurosci.* 2, 539–550.
- Sauseng, P., Klimesch, W., Gruber, W.R., Hanslmayr, S., Freunberger, R., Doppelmayr, M., 2007. Are event-related potential components generated by phase resetting of brain oscillations? A critical discussion. *Neuroscience* 146, 1435–1444.
- Schroeder, C., Lakatos, P., 2009. Low-frequency neuronal oscillations as instruments of sensory selection. *Trends Neurosci.* 32, 9–18.
- Shah, A.S., Bressler, S.L., Knuth, K.H., Ding, M., Mehta, A.D., Ulbert, I., Schroeder, C.E., 2004. Neural dynamics and the fundamental mechanisms of event-related brain potentials. *Cereb. Cortex* 14, 476–483.
- Siegel, M., Donner, T.H., Oostenveld, R., Fries, P., Engel, A.K., 2008. Neuronal synchronization along the dorsal visual pathway reflects the focus of spatial attention. *Neuron* 60, 709–719.
- Sprent, P., 1998. *Data Driven Statistical Methods*. Chapman & Hall, London.
- Tallon-Baudry, C., Bertrand, O., Peronnet, F., Pernier, J., 1998. Induced gamma-band activity during the delay of a visual short-term memory task in humans. *J. Neurosci.* 18, 4244–4254.
- Vanni, S., Revonsuo, A., Hari, R., 1997. Modulation of the parieto-occipital alpha rhythm during object detection. *J. Neurosci.* 17, 7141–7147.
- Vanni, S., Warnking, J., Dojat, M., Delon-Martin, C., Bullier, J., Segebarth, C., 2004. Sequence of pattern onset responses in the human visual areas: an fMRI constrained VEP source analysis. *Neuroimage* 21, 801–817.
- Womelsdorf, T., Fries, P., 2007. The role of neuronal synchronization in selective attention. *Curr. Opin. Neurobiol.* 17, 154–160.
- Wright, R.D., Ward, L.M., 2008. *Orienting of Attention*. Oxford University Press, New York, NY.
- Yamagishi, N., Callan, D.E., Goda, N., Anderson, S.J., Yoshida, Y., Kawato, M., 2003. Attentional modulation of oscillatory activity in human visual cortex. *Neuroimage* 20, 98–113.
- Yeung, N., Bogacz, R., Holroyd, C.B., Cohen, J.D., 2004. Detection of synchronized oscillations in the electroencephalogram: an evaluation of methods. *Psychophysiology* 41, 822–832.